Progress Report for the 2005 SCEC Project

# Analysis of spatio-temporal strain patterns associated with southern California earthquakes

PI: Thorsten W Becker
University of Southern California

Category: B. Integration and Theory
Disciplinary groups: Seismology, Fault and Rock Mechanics
Focus areas: Fault Systems

## Summary

SCEC funding for 2005 was provided to us in order to study small-event seismic strain accumulation in southern California using summation of focal mechanisms. The first project year has focused on the training of a new graduate student at USC, Iain Bailey, the development of a computational foundation with which to apply our methods, analysis of general patterns, and critical evaluation of input data. We are now in a position where we can rapidly create a strain tensor catalog for individual events or for sub-volumes of a crustal block. This method allows us to evaluate the existence and possible variations of strain-release patterns over different length, time, and magnitude scales. We presented this work at two meetings [1, 2], will present again at Fall AGU, and foresee the completion of publishable work from this line of research within the next few months. A minor fraction of the SCEC funding was also used to supplement support of a M.Sc. student at USC, Katrin Plenkers, to conduct research on stress inversion methods that will complement our main strain summation study.

## Main project: Strain summation

### Methodology and Objective

While GPS networks and InSAR surveys provide a quantitative description of present-day crustal deformation on the Earth's surface, they provide few precise constraints upon deformation at seismogenic depths. We are, however, able to collect information from individual earthquakes, and we can think of each event as a strainmeter within the crust [*e.g.,* 3–9]. Our approach is to approximate events with a point-source double couple, and use the associated fault plane solution parameters (strike, dip and rake) to calculate the corresponding potency tensor, $P_{ij}$ [10]. Also required for this computation is the scalar potency, $P_0$, which is calculated via empirical relations [11]. Our use of potency, which is related to moment via the relation $M_0 = \mu P_0$, is simply to emphasize that we are making no assumptions about material rigidity, $\mu$. By summation of all potency tensors within a given volume and over a certain time period, we are able to characterize the net seismic strain release within the summed region by a single, symmetric tensor; a procedure known as Kostrov [5] summation. We can assess the generality or meaning of this tensor by adjustment of the selection region's (or bin's) defining parameters (spatial and temporal (4-D) extent, as well as the magnitude range of included earthquakes), and also by comparison with a method where the summation is unweighted with regard to the event size (*i.e.* we set $P_0 \equiv 1$ for all events in the summation).

A comprehensive characterization of strain release patterns throughout the seismogenic crust will be important for our understanding of crustal stress patterns, mapping of fault zone structure at depth, and the degree of heterogeneity in large, plate boundary fault systems. During the past year we have continued, with this goal in mind, to develop a method of studying 4-D strain release using focal mechanism data for the southern California. We specifically target small-scale seismicity, where the sampling is spatially and temporally extensive, and the large event numbers allow patterns to emerge above natural fluctuations and noise of the data. Our progress over the first year can be broken down into five distinct parts: development of the computational infrastructure, visual assessment of the predominant patterns, analysis of potential artifacts caused by the method, critical evaluation of the catalog data input, and statistical analysis of focal mechanism patterns. A summary of our key findings is presented below.

### Progress

**Development of computational tools** The initial stages of this work concentrated on the development of a computer program that would allow us to flexibly input focal mechanism data, and rapidly create a catalog of

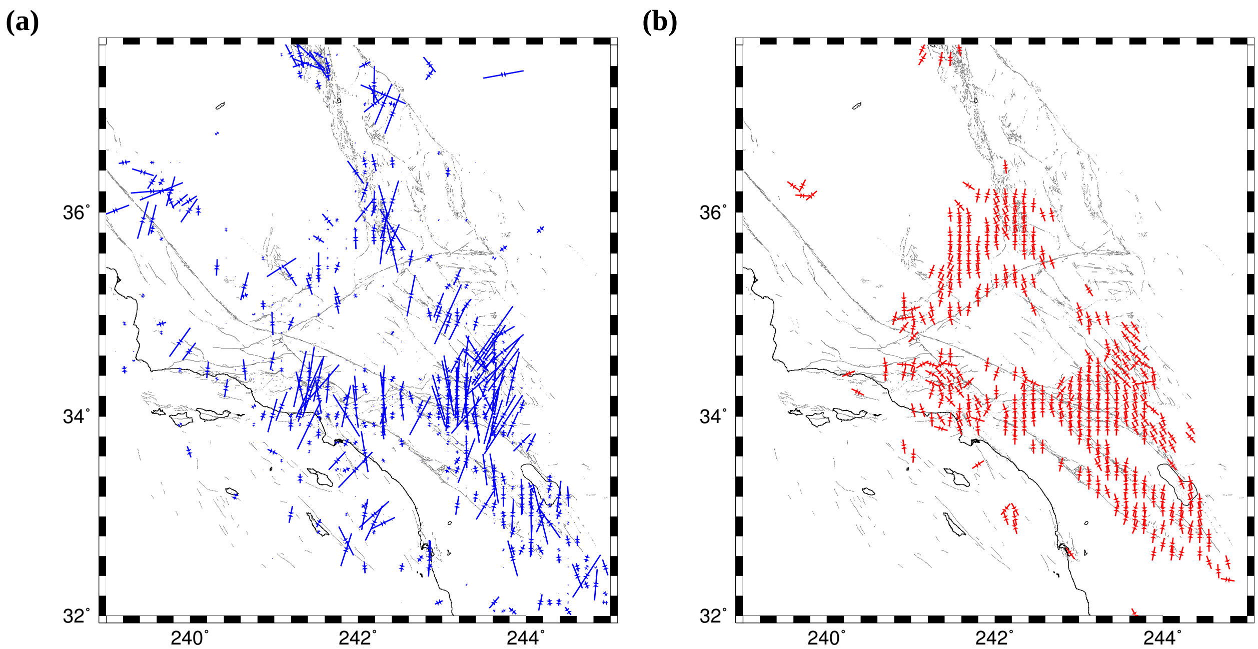


**Figure 1:** Horizontal component of seismic strain release in southern California using potency weighted (a), and potency unweighted (normalized, b) summation for 10×10 km vertical column bins and EH00 catalog data. In the potency weighted case, length of sticks scales with the logarithm of horizontal component of the maximum (compressive) eigenvalue, arbitrary units. In the potency unweighted summation, $P_0 \equiv 1$ for all events, and only bins with 10 or more events are plotted. Fault traces are from [13].

summed (or individual) potency tensors that can be graphically or numerically analyzed. We are currently at a stage where we can divide a crustal block into a three dimensional rectangular grid, with elements retaining equal volume, and create our catalog of summed tensors. Initial results from this procedure were presented at the Spring 2005 SSA meeting [1], and example outputs from this program are shown in Figure 1, and may be compared to, *e.g.*, Becker et al.'s [12] strain and stress plots.

Fault plane solution data are available for between ∼20,000 and ∼96,000 events over the consistently instrumented catalog duration from 1980 to 2004, depending on restrictions with regard to data quality. Subdivision of the region into spatial bins yields a power law distribution of events per bin *vs.* number of events. For example, a 10×10 km lateral division of the entire catalog gives a maximum bin event number of up to ∼5,000.

**First order analysis of dominant patterns** Our initial computational work allowed us to get an idea of the patterns and dominant mechanisms shown by the data to a first order approximation. We found that summed tensors are, as expected, dominated by the largest event included in the summation. In contrast, a potency unweighted summation is dominated by the more numerous small events, which are often the aftershock sequences that also cannot be thought of as independent of the largest event. Far from being an area of concern, this is a point of interest. We can analyze these effects by comparison of the potency unweighted and weighted results, as well as progressively decreasing our upper magnitude cutoff for aftershock dominated regions (*e.g.* Landers, North Ridge) and regions with more constant and consistent seismicity patterns

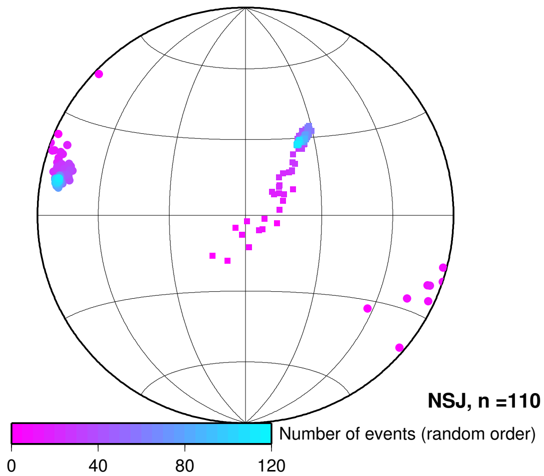


**Figure 2:** Estimated mean orientation for the principle strain axes based on a successively increasing number of events from a $10 \times 10$ km bin at the northern end of the San Jacinto Fault (Schmidt projection). The data were randomized from the catalog temporal sequence; yet, they show an apparent shift in the mean of the intermediate axis. Such effects illustrate the statistical uncertainties in the strain summations, and will be evaluated further so as to be able to put error bounds on estimated temporally changing signals.

(*e.g.* the central San Jacinto Fault Zone). Initial results of an analysis of such features were presented at the 2005 SCEC meeting [2]. We discussed the consistency and discrepancies between results based on different summing and bin-averaging methods, and how these features vary regionally.

**Analysis of data reliability** We are wary of basing conclusions on results produced by a technique that involves a number of assumptions and approximations, without fully examining the effects of this method. In our work presented at the SCEC conference, we found that a significant number of events are needed to remove minor temporal fluctuations or artifacts from the summation process (Figure 2). To study the effect of a specific bin's selection criteria upon the summed tensor, we obviously need as many events as possible in all directions over all time. We therefore moved to increase our input fault plane solution data set with a preference for quantity rather than quality [15]. The idea is to exploit small event strain accumulation and examine how small scale ($\sim$ 5 km) patterns merge with the larger, tectonic variations ($\sim$50 km).

Previously, we had been making use of the Hauksson catalogs [16], which are available via the SCEDC website and calculated using FPFIT [17]. However, the public version of this catalog displays variations in magnitude and gaps in the catalog (Figure 3). Those would disappear if the catalog would be recompiled [E. Hauksson, pers. comm.]; to avoid such artifacts and to have better control over the quality criteria, we have therefore moved to create our own catalogs, following Hauksson's [16] approach.

Our initial attempts at producing a catalog with a larger number of fault plane solutions used a simple 1D velocity model [19], and restricted the quality solely by the minimum number of first arrival picks needed (set to nine). Although we expect the quality to be lower, increased scatter should not be a problem as long as errors remain unbiased, which we will test. However, decreasing the restrictions applied to the FPFIT method did lead to a clear bias towards certain solutions (Figure 4). We are currently working to isolate the source of these artifacts, while simultaneously developing a catalog using the alternative HASH program [18] for comparison.

**Statistical analysis of focal mechanism patterns** In the process of examining our primary data in more detail, we have also begun to study the spatial distribution of the principle strain axes for all earthquakes. Given the approximations we make about the earthquake sources, these axes are coincident with the focal mechanism P, T and null axes. When considering fault plane solutions from three different catalogs, we find a noticeable difference in the patterns observed (Figure 4). Once methodological problems are fixed,

**Figure 3:** Comparison of catalogs (magnitude *vs.* time) by Hauksson [16] (EH00, updated from the SCECDC), Hardebeck and Shearer [18] (HASH), and our own catalog. EH00 uses a minimum number of picks of 12, is a composite of four files, and the velocity model used for inversions is continuously updated. HASH uses first arrivals and *S*/*P* amplitude ratios and a minimum of eight picks, with stringent quality criteria for takeoff angle and azimuthal gaps, and an evaluation of robustness with respect to velocity models. Our catalog is modeled after EH00 and computed with FPFIT [17] using a minimum of nine picks and a simple a 1-D velocity model [19].

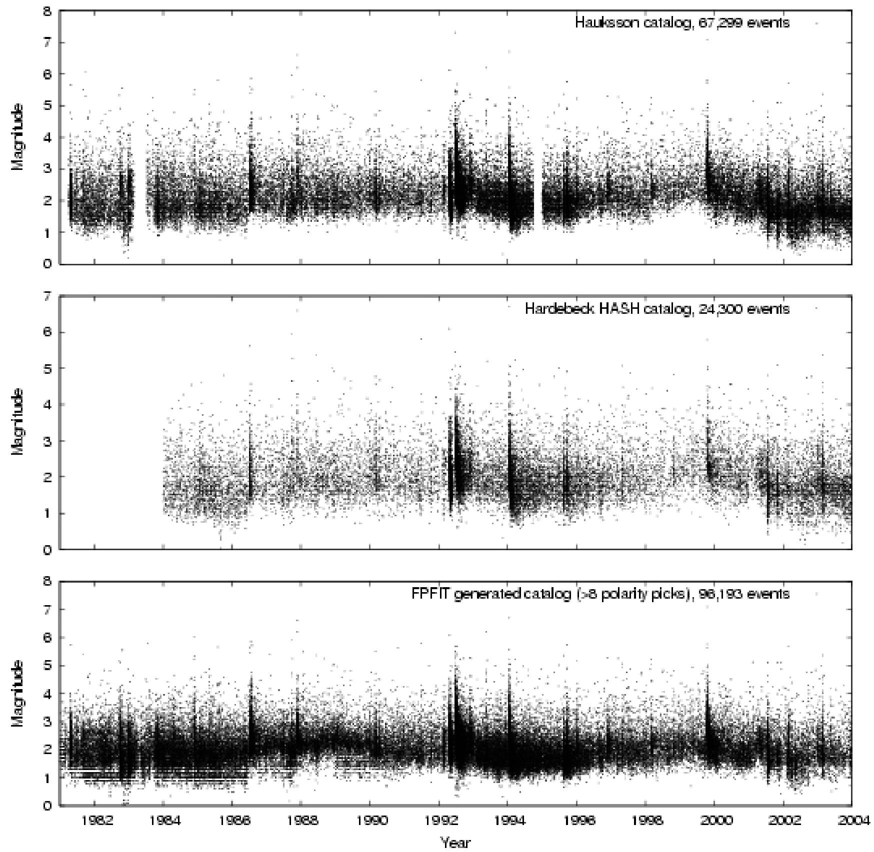


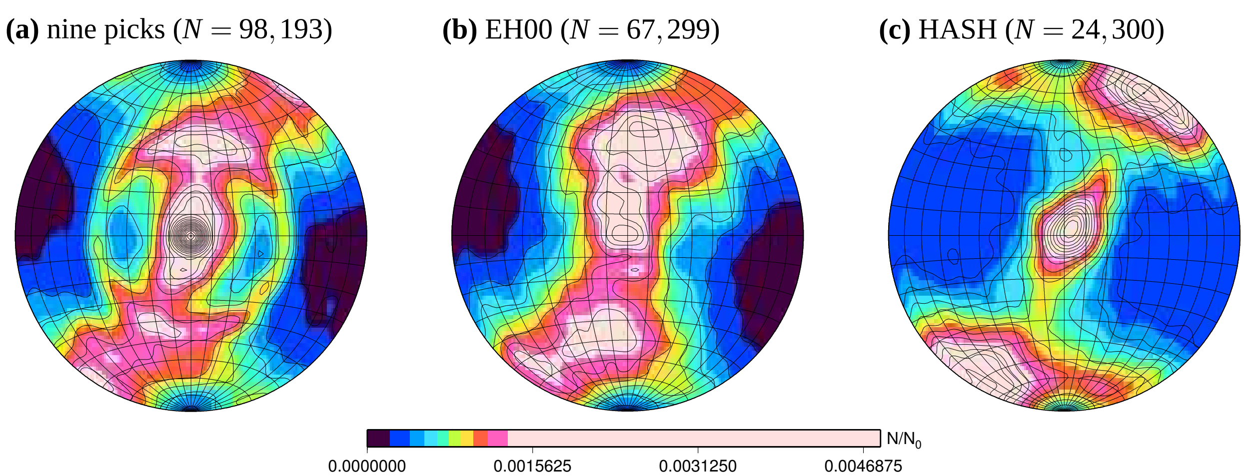


**Figure 4:** Summed orientations of the individual, principal compressive eigenaxis of our FPFIT catalog (a), EH00 (b), and HASH (c) on a equal-area stereo net. North and East are up and right in the plot, respectively, with center indicating vertical axis (Schmidt projection). Shading is by normalized cell count (total number $N$ given in title) and smoothed equally for (a) – (c). The nine pick catalog shows a clear preference for 45 or 90° plunge of the axes, showing that quality restrictions must be increased in our use of FPFIT.

our continuing work will be to study the orientation statistics and how they change in regions dominated by different faulting styles, and apparent differences in complexity [*cf.* 20].

### Minor project: Tests of stress inversion methods

Often, the tectonic stress field in the Earth's crust is inferred from focal mechanism solutions by means of stress inversions [*e.g.* 20–27]. However, results and their error estimates are still debated [29, 8, 30, 31, 32]. As it is typically impossible to directly compare results from stress inversions with the true stress regime, the robustness of the results is hard to evaluate based on data alone. In particular the detailed tectonic setting and the material parameters of the Earth's crust (*e.g.* the coefficient of friction), which are necessary inputs for some stress inversion methods, are not well known but may have a large effect [29, 33, 31]. To address the related issues of stress *vs.* strain inversions in the presence of material heterogeneity, we perform a comprehensive numerical modeling test of stress inversion methods. We generate synthetic focal mechanisms in a 3-D boundary element code, taking into account step-by-step the effect of different parameters and assumptions about fault behavior and friction laws. In this fashion, it should be possible to test to what extent the crustal stress may be detected under which assumptions by different inversion methods.

We have initially focused on comparing results from the widely used stress inversion methods by Michael [21, 34] and Gephart and Forsyth [22, 35]. Michael's approach is a linear inversion method, whereas as Gephart's is based on a nonlinear inversion algorithm. Assisted by the PI, Ms. Plenkers has obtained, compiled, and tested these algorithms and is now in the process of applying such inversion methods to synthetic data. To generate synthetics, we model earthquake interactions within the quasi-static approximation using the displacement discontinuity method [36], based on dislocation routines by Okada [37] in the implementation of [38]. The model simulates a purely elastic half-space with preexisting fault planes and a stress tensor acting on the fault system. The model output is the time and the orientation of slip on discretized patches, where failure is computed based on simple friction laws. We will vary this model's parameters systematically, for example by changing the friction law which is used to describe the rupture process, the geometry of the faults, and possible anisotropy in fault strength, or friction.

### Publications sponsored through this grant

- I. Bailey, T. W. Becker, and Y. Ben-Zion (2005a): Patterns of crustal coseismic strain release associated with different earthquake sizes as imaged by a tensor summation method. In *2005 SCEC Annual Meeting Abstracts*, page 9, Los Angeles, CA. Southern California Earthquake Center. Available online at `http://www.scec.org/meetings/2005am/2005abstracts.doc`.

- I. W. Bailey, T. W. Becker, and Y. Ben-Zion (2005b): Strain release in southern California based on earthquake catalog data (abstract). *Seis. Res. Lett.*, 76 (2).

## References


[1] I. Bailey, T. W. Becker, and Y. Ben-Zion. Patterns of crustal coseismic strain release associated with different earthquake sizes as imaged by a tensor summation method. In *2005 SCEC Annual Meeting Abstracts*, page 9, Los Angeles, CA, 2005. Southern California Earthquake Center. available online at `http://www.scec.org/meetings/2005am/2005abstracts.doc`.

[2] I. W. Bailey, T. W. Becker, and Y. Ben-Zion. Strain release in southern california based on earthquake catalog data (abstract). *Seis. Res. Lett.*, 76(2), 2005.

[3] K. Aki. Generation and propagation of G waves from the Niigata earthquake of June 16 1964. 2. Estimation of earthquake movement released energy and stress-strain drop from G wave spectrum. *Bull. Earthq. Res. Inst. Tokyo Univ.*, 44:23–88, 1966.

[4] J. N. Brune. Seismic moment seismicity and rate of slip along major fault zones. *J. Geophys. Res.*, 73: 777–784, 1968.

[5] B. V. Kostrov. Seismic moment and energy of earthquakes and seismic flow of rock. *Phys. Solid Earth*, 1:23–40, 1974.

[6] K. M. Fischer and T. H. Jordan. Seismic strain rate and deep slab deformation in Tonga. *J. Geophys. Res.*, 96:14429–14444, 1991.

[7] F. Amelung and G. C. P. King. Large-scale tectonic deformation inferred from small earthquakes. *Nature*, 386:702–705, 1997.

[8] R. J. Twiss and J. R. Unruh. Analysis of fault slip inversions: Do they constrain stress or strain rate? *J. Geophys. Res.*, 103:12205–12222, 1998.

[9] S. A. Sipkin and P. G. Silver. Characterization of the time-dependent strain field at seismogenic depths using first-motion focal mechanisms: Observations of large-scale decadal variations in stress along the San Andreas Fault system. *J. Geophys. Res.*, 108(doi:10.1029/2002JB002064), 2003.

[10] K. Aki and P. G. Richards. *Quantitative Seismology*, volume 1. Freeman and Company, New York, 1980.

[11] Y. Ben-Zion and L. Zhu. Potency-magnitude scaling relations for southern california earthquakes with $1.0 < M_L < 7.0$. *Geophys. J. Int.*, 148:F1–F5, 2002.

[12] T. W. Becker, J. L. Hardebeck, and G. Anderson. Constraints on fault slip rates of the southern California plate boundary from GPS velocity and stress inversions. *Geophys. J. Int.*, 160:634–650, 2005.

[13] C. W. Jennings. *Fault map of California with locations of volcanoes, thermal springs, and thermal wells*. Number 1 in Geologic Data Map. California Division of Mines and Geology, Sacramento CA, 1975.

[14] N. I. Fisher, T. Lewis, and B. J. J. Embleton. *Statistical Analysis of Spherical Data*, volume 1. Cambridge University Press, New York, 1987.

[15] D. Kilb and J. Hardebeck. Fault parameter constraints using relocated earthquakes: A validation of first motion focal mechanism data. *Bull. Seismol. Soc. Am.*, 2005. submitted.

[16] E. Hauksson. Crustal structure and seismicity distribution adjacent to the Pacific and North America plate boundary in southern California. *J. Geophys. Res.*, 105:13875–13903, 2000.

[17] P. Reasenberg and D. Oppenheimer. FPFIT, FPPLOT, and FPPAGE: FORTRAN computer programs for calculating and displaying earthquake fault-plane solutions. *U. S. Geological Survey Open File Report*, 85-739:109, 1985.

[18] J. L. Hardebeck and P. M. Shearer. Using S/P amplitude ratios to constrain the focal mechanisms of small earthquakes. *Bull. Seismol. Soc. Am.*, 93:2434–2444, 2003.

[19] D. Hadley and H. Kanamori. Seismic structure of the Transverse Ranges. *Geol. Soc. Am. Bull.*, 88: 1469–1478, 1977.

[20] J. Hardebeck. Homogeneity of small-scale earthquake faulting, stress and fault strength. In *2005 SCEC Annual Meeting Abstracts*, page 145, Los Angeles, CA, 2005. Southern California Earthquake Center.

available online at `http://www.scec.org/meetings/2005am/2005abstracts.doc`.

[21] A. J. Michael. Determination of stress from slip data; faults and folds. *J. Geophys. Res.*, 89:11517–11526, 1984.

[22] J. W. Gephart and D. W. Forsyth. An improved method for determining the regional stress tensor using earthquake focal mechanism data: Application to the San Fernando earthquake sequence. *J. Geophys. Res.*, 89:9305–9320, 1984.

[23] L. Rivera and A. Cisternas. Stress tensor and fault plane solution for a population of earthquakes. *Bull. Seismol. Soc. Am.*, 80:600–614, 1990.

[24] T. Plenefisch and K.-P. Bonjer. The stress field in the Rhine Graben area inferred from earthquake focal mechanisms and estimation of frictional parameters. *Tectonophysics*, 275:71–97, 1997.

[25] G. A. Abers and J. W. Gephart. Direct inversion of earthquake first motions for both the stress tensor and focal mechanisms and application to southern California. *J. Geophys. Res.*, 106:26523–26540, 2001.

[26] J. L. Hardebeck and E. Hauksson. Crustal stress field in southern California and its implications for fault mechanics. *J. Geophys. Res.*, 106:21859–21882, 2001.

[27] S. Prejean, W. Ellsworth, M. Zoback, and F. Waldhauser. Fault structure and kinematics of the Long Valley Caldera region, California; revealed by high-accuracy earthquake hypocenters and focal mechanism stress inversion. *J. Geophys. Res.*, 107(doi:10.1029/2001JB001168):2355, 2002.

[28] J. Townend and M. D. Zoback. Regional tectonic stress near the San Andreas fault in central and southern California. *Geophys. Res. Lett.*, 31(doi:10.1029/2003GL018918), 2004.

[29] D. D. Pollard, S. D. Saltzer, and A. Rubin. Stress inversion methods: are they based on faulty assumptions? *J. Struct. Geol.*, 15:1045–1054, 1993.

[30] J. L. Hardebeck and E. Hauksson. Stress orientations obtained from earthquake focal mechanisms; what are appropriate uncertainty estimates? *Bull. Seismol. Soc. Am.*, 91:250–262, 2001.

[31] D. E. Smith and T. H. Heaton. Interpreting focal mechanisms in a heterogeneous stress field (abstract). *EOS Trans. AGU*, 84(46):S41C–0105, 2003.

[32] P. Xu. Determination of regional stress tensors from fault-slip data. *Geophys. J. Int.*, 157:1316–1330, 2004.

[33] L. Rivera and H. Kanamori. Spatial heterogeneity of tectonic stress and friction in the crust. *Geophys. Res. Lett.*, 29(doi:10.1029/2001GL013803), 2002.

[34] A. J. Michael. Use of focal mechanisms to determine stress; a control study. *J. Geophys. Res.*, 92:357–368, 1987.

[35] J. W. Gephart. Stress and the direction of slip on fault planes. *Tectonics*, 9:845–858, 1990.

[36] S. L. Crouch and A. M. Starfield. *Boundary Element Methods in Solid Mechanics. With Applications in Rock Mechanics*. Allen and Unwin, London, 1983.

[37] Y. Okada. Internal deformation due to shear and tensile faults in a half-space. *Bull. Seismol. Soc. Am.*, 82:1018–1040, 1992.

[38] T. W. Becker and B. Schott. On boundary-element models of elastic fault interaction (abstract). *EOS Trans. AGU*, 83(47):NG62A–0925, 2002.